Journal of Instrumentation

PAPER • OPEN ACCESS

Spectroscopic effects of distributed-line phenomena in integrated feedback resistors for charge-sensitive pre-amplifiers

To cite this article: S. Capra *et al* 2024 *JINST* **19** C01029

Published by IOP Publishing for Sissa Medialab

Received: *September 30, 2023*
Revised: *November 17, 2023*
Accepted: *November 20, 2023*
Published: *January 18, 2024*

24th International Workshop on Radiation Imaging Detectors
Oslo, Norway
25–29 June 2023

2024 JINST 19 C01029

Spectroscopic effects of distributed-line phenomena in integrated feedback resistors for charge-sensitive pre-amplifiers

S. Capra,* G. Secci and A. Pullia

[a] *Dipartimento di Fisica "Aldo Pontremoli", Università degli Studi di Milano, Via Celoria 16, Milano, Italy*
[b] *INFN, Sezione di Milano, Via Celoria 16, Milano, Italy*

E-mail: stefano.capra@unimi.it

Abstract: The distributed capacitive coupling of high-valued resistors with ground planes modifies their effective impedance and power spectral density of noise, especially at high frequency. This effect is clearly visible in poly-silicon resistors inside integrated circuits. When such resistors are used in the feedback network of Charge Sensitive Pre-amplifiers an excess noise arises with a non-white noise spectral density. The effect is a worsening of the spectroscopic resolution. The relevance of such effect with respect to the conventional noise sources is discussed in different practical cases.

Keywords: Analogue electronic circuits; Front-end electronics for detector readout

*Corresponding author.

https://doi.org/10.1088/1748-0221/19/01/C01029

Contents

1 Introduction

Charge-sensitive pre-amplifiers (CSP) for semiconductor radiation detectors require a feedback discharge device to ensure proper functionality and avoid saturation. This can be a continuous-time device, like a simple resistor or trans-conductor, or an active structure that provides pulsed reset [1, 2]. Traditionally in the field of gamma spectroscopy such device is a discrete resistor of high value (1 GΩ or more) [3, 4]. This because the noise produced by this device is one of the key elements that concur in defining the total equivalent input noise of the pre-amplifier. For the same reason this device can be operated at liquid nitrogen temperature for noise minimization. The state-of-the-art spectroscopic filtering techniques require also this device to be exceptionally linear in order to produce exponential-shaped signals at the pre-amplifier output to ensure best energy resolution. Unfortunately such surface-mount devices are realized on ceramic substrates that are not radio-pure and this can be an issue if radio-purity is required, like in underground laboratories where rare-decay studies are carried out [5]. Such devices are also bulky and may be an issue while pursuing maximum system integration in high-channel-number applications. Since active trans-conductors generally have a higher noise respect to passive resistors, integrated high-resistivity polysilicon resistors seem a viable solution to combine integration, low noise and radio-purity. In fact, silicon dies are naturally radio-pure due to their technological production process. One factor that should not be underestimated is the capacitive coupling to bulk that characterize such integrated polysilicon resistors. Such capacitance turn integrated polysilicon resistors into distributed-line devices. The interaction of the resistor thermal noise with such distributed capacitance shapes the white power spectral density of noise that such resistor produces when connected as feedback device of charge-sensitive pre-amplifier [6]. Interestingly, the net effect is the appearance of a current noise component with power spectral density proportional to the square root of frequency. When conventional spectroscopy shaping techniques are applied to the signals from charge-sensitive amplifiers equipped with such resistor, an equivalent noise charge component arises that is proportional to the square root of the shaping time [7]. Quantitative examples of realistic use-cases are given.

2 Circuit description

Let's consider the simplified spectroscopic chain of figure 1, where pre-amplifier and shaping amplifier are condensed into a single block with transfer function $S(f)$ defined as the ratio between the output voltage and the input current. The voltage generators v^2_{white} and $v^2_{1/f}$ describe the white thermal noise and the 1/f noise of the pre-amplifier input transistor. On the other side, i^2_{white} takes into account the shot noise of the input transistor and that of the detector. A second current generator is outlined: i^2_{RWDC}. It describes both the white and non-white noise (the one whose power spectral density is proportional to the square root of the frequency) introduced by the resistor with distributed capacitance (RWDC). The capacitor C_{TOT} sums up the detector capacitance, the feedback capacitance, the pre-amplifier input transistor capacitance and all the input node-referred stray capacitance.

The Equivalent Noise Charge (ENC) of the electronic spectroscopic chain is given by [7]:

$$ENC^2 = (a + a' \cdot K_1) \cdot \Omega_1 \cdot \tau + b \cdot \Omega_2 + c \cdot \frac{\Omega_3}{\tau} + d \cdot K_4 \cdot \Omega_4 \cdot \sqrt{\tau}, \tag{2.1}$$

where a, a', b, c and d are the noise coefficients associated to the above-mentioned noise sources (see [7] for the mathematical expressions). Specifically, a refers to the shot noise, while b and c describe the 1/f and the thermal noise of the input transistor device. On the other hand, a' and d refer to the white and non-white parallel noise introduced by the RWDC on the feedback network. These last two terms are weighted by the K_1 and K_4 coefficients, which are functions of the ratio τ/τ_{RWDC}. We remind the reader that τ is the filter shaping time, while τ_{RWDC} is the noise corner time, defined as:

$$\tau_{\text{RWDC}} = R_{\text{RWDC}} \cdot C_{\text{RWDC}}/2, \tag{2.2}$$

with R_{RWDC} and C_{RWDC} the total resistance and distributed capacitance of the RWDC. From the physical point of view, if $\tau \ll \tau_{\text{RWDC}}$ the white parallel noise of the RWDC is negligible with respect to the non-white noise. Conversely, if $\tau \gg \tau_{\text{RWDC}}$ the RWDC white parallel noise dominates over the non-white one. Ω_1, Ω_2, Ω_3 and Ω_4 depend on the specific shaping amplifier used to improve the CSP signal-to-noise ratio.

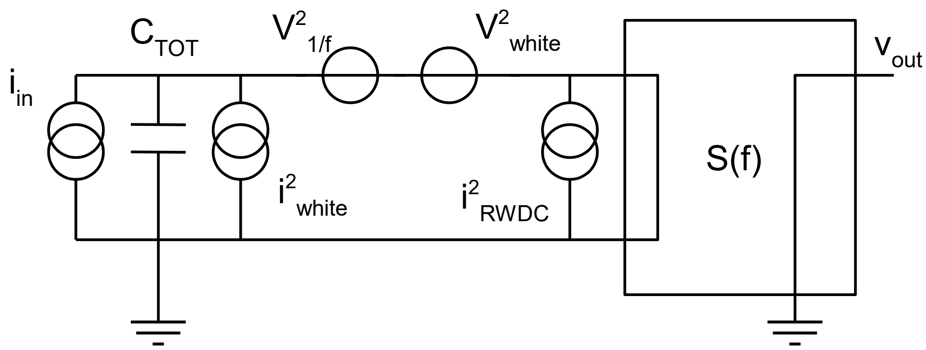

Figure 1. Simplified schematic pointing out the noise sources of a spectroscopic read-out chain.

Two commonly used shaping amplifier are considered: the trapezoidal shaping amplifier, with rise-time equal to the flat-top length, and the Ortec-572 4^{TH} order quasi-Gaussian amplifier [8]. The Ω coefficients for these two filters are summarized in table 1. In the following sections we will

2024 JINST 19 C01029

Table 1. Noise coefficients summary table.

Filter	Ω_1	Ω_2	Ω_3	Ω_4
trapezoidal	1.667	0.2200	0.05066	0.5559
4^{TH}-order quasi-Gaussian	2.025	0.1700	0.02362	0.5365

discuss, starting from the coefficients mentioned above, the net contribution of the RWDC noise both in case of integrated and discrete resistors.

3 The problem of the technological node

The choice of compact integrated solutions for the front-end electronics is mandatory for high-density applications, like for the read-out of highly segmented silicon detectors [9–11]. The minimization of the external discrete components required by the ASICs (Application-Specific Integrated Circuits) may lead for the choice of integrated solutions for the high-valued feedback resistors. It is possible to realize high-valued resistors using high-resistivity polysilicon layers offered by some ASIC technologies like AMS C35 (see [12]). In order to minimize the ENC value it is common practice to choose the highest possible value for the feedback resistor. But is this the right choice when dealing with integrated solutions? In order to give an answer to this question, in figure 2 we compare the ENC vs shaping time plots of the same pre-amplifier with different integrated feedback resistors (20 MΩ, 100 MΩ, 1 GΩ) realized in the same technology with a $\frac{C_{\mathrm{RWDC}}}{R_{\mathrm{RWDC}}}$ ratio of 0.1 pF/MΩ. The difference in spectroscopic resolution between the three cases is counter-intuitively negligible for shaping times under 10 µs, while it becomes appreciable only for very long, ultimately unrealistic, shaping times.

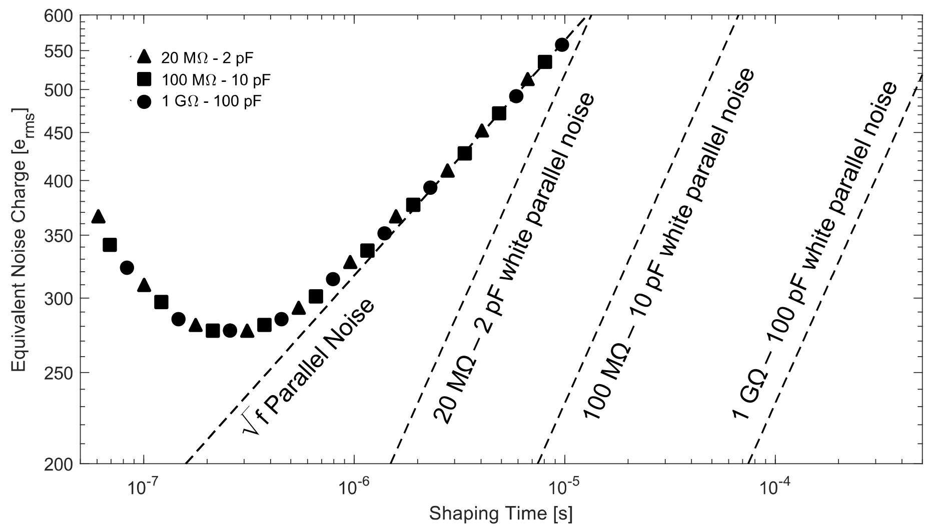

Figure 2. Comparison between the ENC of the same CSP with feedback resistors of 20 MΩ, 100 MΩ and 1 GΩ characterized by the same capacitive coefficient of 0.1 pF/MΩ. The $\tau^{1/4}$ component is equivalent in all the three cases. Trapezoidal shaping with $t_{\mathrm{RISE}} = t_{\mathrm{Flattop}}$, computer simulation.

2024 JINST 19 C01029

As a matter of fact, as described in [6] and [7], the RWDC power spectral density of noise at high frequencies is proportional to $\sqrt{f \cdot C_{\mathrm{RWDC}}/R_{\mathrm{RWDC}}}$. Unfortunately such coefficient is ultimately independent from the choice of the resistor value itself. Once the resistor width has been minimized according to the chosen technology, the total capacitive coupling C_{RWDC} will be proportional to the resistor length, in turn proportional to the resistor value R_{RWDC}. In other words, the ENC^2 component due to the RWDC effect is constant and defined only by the specific ratio between total resistance and total capacitance of the feedback device. It can be lowered only realizing narrower resistors or thicker field oxides, that means essentially choosing a different ASIC technology, since such parameters are not under the designer's control.

4 Are discrete resistors immune to the RWDC issue?

Discrete resistors are generally mounted on insulating ceramic substrates. At the same time, care is taken to avoid strong coupling to grounded metallic planes. For these reasons in first approximation they may seem immune to the issues described so far. The RWDC effect in CSPs with discrete resistor, if present, is submerged under the main conventional noise sources and cannot be experimentally identified. It may be interesting however to estimate its theoretical contribution. The pre-amplifier output node is a low-impedance voltage source. For practical reasons the feedback capacitor and the feedback resistor are generally mounted one close to the other. If the output node is geometrically coupled to the resistor body, it can take the role of a low-impedance voltage reference and produce similar effects in terms of noise, even with very different effects in terms of signal shape. A deeper insight on such phenomena will be topic of future works. A discrete through-hole 1 GΩ resistor can easily be 2-3 mm wide and 7-8 mm long. A in-air capacitor of area 5 mm^2 and plate distance of 2 mm has a total capacitance of 22 fF. In figure 3 the ENC contribution of a 1 GΩ resistor is plotted against shaping time for different values of capacitive coupling, in the approximation of constant coupling across the whole resistor body. The RWDC effect is very subtle: its excess noise adds up in the region where normally the 1/f noise is the main contributor.

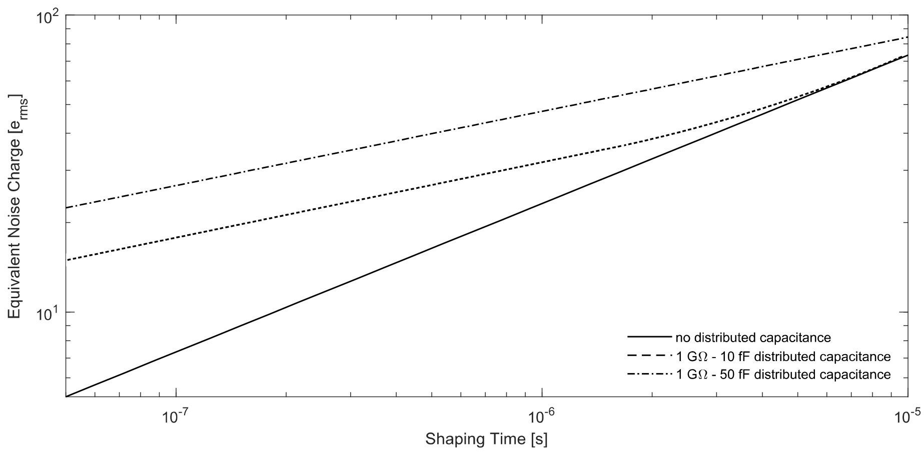

Figure 3. ENC comparison between 1 GΩ resistor with no distributed capacitance, 1 GΩ resistor with 10 fF distributed capacitance and 1 GΩ resistor with 50 fF distributed capacitance. Simulations were performed considering trapezoidal shaping with $t_{\mathrm{RISE}} = t_{\mathrm{Flattop}}$.

5 Conclusions

Even if it may seem absolutely counter-intuitive, there is no practical difference in the ENC of an integrated charge-sensitive pre-amplifier equipped with integrated polysilicon resistors with values between 20 MΩ and 1 GΩ with coupling factor of 0.1 pF/MΩ. The only way to reduce further the ENC is to act directly on the coupling factor itself which is not design dependent but technology dependent. The estimation of the RWDC effect in large, discrete resistors is extremely subtle and can be mostly submerged by the contribution of the series 1/f noise.

References

[1] D.A. Landis, F.S. Goulding, R.H. Pehl and J.T. Walto, *Pulsed feedback tecniques for semicondctor detector radiation spectrometers*, IEEE Trans. Nucl. Sci. **18** (1971) 115.

[2] F. Mele, M. Gandola and G. Bertuccio, *SIRIO: A High-Speed CMOS Charge-Sensitive Amplifier for High-Energy-Resolution X-γ Ray Spectroscopy With Semiconductor Detectors*, IEEE Trans. Nucl. Sci. **68** (2021) 379.

[3] S. Capra and A. Pullia, *Design and experimental validation of an integrated multichannel charge amplifier for solid-state detectors with innovative spectroscopic range booster*, IEEE Trans. Nucl. Sci. **67** (2020) 1877.

[4] A. Pullia, F. Zocca and S. Capra, *Note: A 102 db dynamic-range charge-sampling readout for ionizing particle/radiation detectors based on an application-specific integrated circuit (ASIC)*, Rev. Sci. Instrum. **89** (2018) 026107.

[5] GERDA collaboration, *Searching for neutrinoless double-beta decay with GERDA*, Nucl. Instrum. Meth. A **958** (2020) 162112.

[6] S. Capra, *Impedance and Noise Closed-Form Model of Large-Area Integrated Resistors With High Stray Capacitance to be Used as Feedback Discharge Devices in Charge-Sensitive Preamplifiers for Nuclear Spectroscopy*, IEEE Trans. Nucl. Sci. **67** (2020) 722.

[7] S. Capra, G. Secci and A. Pullia, *Equivalent noise charge contribution of the* $\sqrt{f}$ *parallel noise in nuclear spectroscopic measurements using different shaping amplifiers*, IEEE Trans. Nucl. Sci. **70** (2023) 730.

[8] ORTEC, *ORTEC 572A Amplifier*, https://www.ortec-online.com/products/electronics/amplifiers/572a.

[9] S. Capra et al., *Performance of the new integrated front-end electronics of the trace array commissioned with an early silicon detector prototype*, Nucl. Instrum. Meth. A **935** (2019) 178.

[10] A. Castoldi, C. Guazzoni and T. Parsani, *Versatile multi-channel CMOS frontend with selectable full-scale dynamics from 100 MeV up to 2.2 GeV for the readout of detector's signals in nuclear physics experiments*, Nuovo Cim. C **41** (2018) 168.

[11] S. Capra et al., *Design of an integrated low-noise, low-power charge sensitive preamplifier for γ and particle spectroscopy with solid state detectors*, in the proceedings of the *2014 IEEE Nuclear Science Symposium and Medical Imaging Conference (NSS/MIC)*, Seattle, WA, U.S.A. (2014), p. 1–4 [DOI:10.1109/NSSMIC.2014.7431043].

[12] AMS home page, https://ams.com (Accessed September 2023).

2024 JINST 19 C01029